RAMAN LIDAR DEDICATED TO WATER VAPOR MEASUREMENTS IN THE LOWER TROPOSPHERE (WALINEAS)

Frédéric Laly [a,b], **Patrick Chazette**[a], **Julien Totems**[a], **Jérémy Lagarrigue**[a], **Cyrille Flamant**[c]

[a]*LSCE/IPSL, CNRS-CEA-UVSQ, University Paris-Saclay, CEA Saclay, Gif sur Yvette, France*
[b]*ADDAIR Company, 78530, Buc, France*
[c]*LATMOS/IPSL, CNRS-SU-UVSQ, Sorbonne Université, Paris, France Paris, France*
Lead Author e-mail address: frederic.laly@lsce.ipsl.fr

Abstract: Climate change is already leading to significant changes in rainfall patterns in the Mediterranean basin, and particularly in the south of France. The resilience of local population to extreme precipitation events requires investigative means of water vapor variability in the lower troposphere with high spatio-temporal resolution such as Raman lidar, associated to state-of-the-art weather models. This is the aim of the Water Vapor Lidar Network Assimilation (WaLiNeAs) research program, which was supported by France to carry out a demonstration campaign in autumn and winter 2022-2023.

1 INTRODUCTION

The Mediterranean Basin has been identified as a hotspot of climate change for the years to come, as its population is expected to increase to 500 million inhabitants within the next 15 years [1]. In the context of global warming, this area has increasingly been subjected to heavy precipitation events (HPEs) that produce flash floods and landslides during autumn (e.g. [2]).

Humid air masses from the Atlantic Ocean and Saharan regions are advected over the Mediterranean Sea and reach the coast of southern France, which leads to HPEs [3]. It has already been established experimentally that before HPEs, the atmosphere is moister, with an increase in water vapor content in the first kilometres above ground level [4]. By this way, [5] used data acquired by a ground-based Raman lidar in the Balearic Islands along with satellites data to study the formation of mesoscale convective systems which impacted the Cevennes–Vivarais area as they lead to HPEs.

We present here the French component of the WaLiNeAs ground-based campaign, the database built from Raman lidar measurements performed in autumn and winter 2022-2023, and the main characteristics of the moisture profiles in relation with the encountered weather conditions.

1.1 WaLiNeAs ground-based campaign

The main objective of the WaLiNeAs campaign is to improve the prediction of HPEs and the understanding of the initial conditions that generate these events by assimilating the water vapor mixing ratio (WVMR) derived from Raman lidar measurements into mesoscale models. The associated field campaign involved 4 European countries operating 8 ground-based stations equipped with Raman lidars along the western Mediterranean basin.

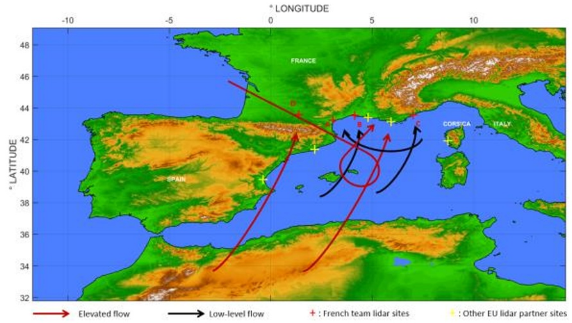

Fig. 1. Map of the WaLiNeAs campaign lidar sites and of the main flow patterns below 2 km (black arrows) and between 2 and 4 km (brown arrows).

The work that will be presented focuses on the 3 ground-based Raman lidar stations operated by the French component of WaLiNeAs at Cannes

(43°32’29’’N 6°57’30’’E), Grau-du-Roi (43°31’14’’N 4°7’39’’E) and Coursan (43°14’5’’N 3°3’49’’E).

The 3 French lidar sites were equipped with [6]: i) the H_2O Raman Ultraviolet Sounder second generation (HORUS–2) at Coursan and Toulouse, ii) the H_2O Raman Ultraviolet Sounder first generation (HORUS–1) at Grau du Roi, and iii) the Water Vapor and Aerosol Lidar (WALI) at Cannes. The sites are indicated by a red cross in Fig. 1. The other lidar sites managed by the different European teams are also shown but as yellow crosses.

1.2 Raman lidars

HORUS is composed of 3 modules to create a compact and autonomous instrument [6]. The electronics module supplies power to the other two modules and contains all the electronics and the optical spectral analyzers, which consist of two rack-mounted fiber optic polychromators. The optics module contains the laser transmitter and the two reception telescopes. Each receiving telescope acquires a N_2–Raman channel and a H_2O–Raman channel to improve the signal to noise ratio.

Inside its field–proof enclosure, the optical architecture of HORUS is almost identical to that of WALI [7,8]. WALI offers the possibility to simultaneously study the aerosol content in the atmosphere, with elastic reception channels, as well as the temperature and water vapor profiles, with rotational and vibrational Raman channels respectively.

1.3 Lidar inversion methodology

The lidar acquires the range-corrected Raman signal S_i from ground level z_G at the altitude a.m.s.l. z of channel i (N_2 or H_2O), of wavelength λ_i (386.6 nm for the dinitrogen channel and 407.5 nm for the water vapor channel). We can then find the WVMR (r_H), according to the following equation [6]:

$$r_H(z) = K_0 \frac{O_N(z)}{O_H(z)} \frac{\langle {}^{S_H(z)}/_{g_H} \rangle_M}{\langle {}^{S_N(z)}/_{g_N} \rangle_M} C_m(z) C_a(z), \qquad (1)$$

Where K_0 is the calibration constant, O_i the overlap factor of channel i, g_i the gain of channel i and C_m and C_a are corrective terms to take account of the presence of aerosols and molecules in the atmosphere. These terms are detailed in [6].

1.4 Calibration

A specific lidar calibration procedure (Fig. 2) was set up and validated in order to overcome the difficulties associated with radiosoundings, where heavy air traffic exists.

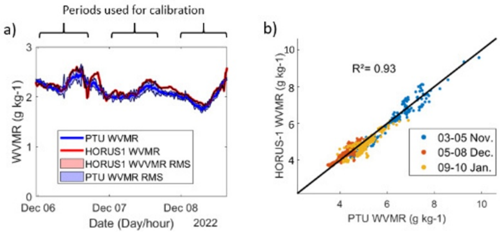

Fig. 2. Examples of time series during which WVMR-derived lidar at 200 m a.g.l. and ground–based weather stations can be considered as equal (left fig.). The correlation between these two independent data types is given in the right figure where the Pearson coefficient is indicated.

The stability over time of the lidar calibrations used was also assessed using radiosonding measurements performed from other sites (Fig. 3).

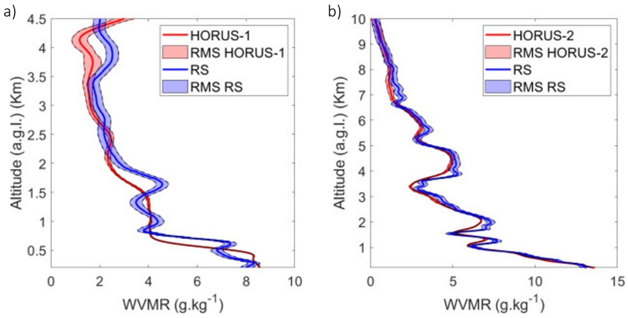

Fig. 3. Examples of cross-comparison of WVMR profiles derived from a) HORUS–1 and a radiosonde (RS) 45 km away and b) HORUS–2 and a coincident RS. The coloured area gives the standard deviation around the mean value.

2 RESULTS AND DISCUSSION

2.1 Temporal evolution of the WVMR profile

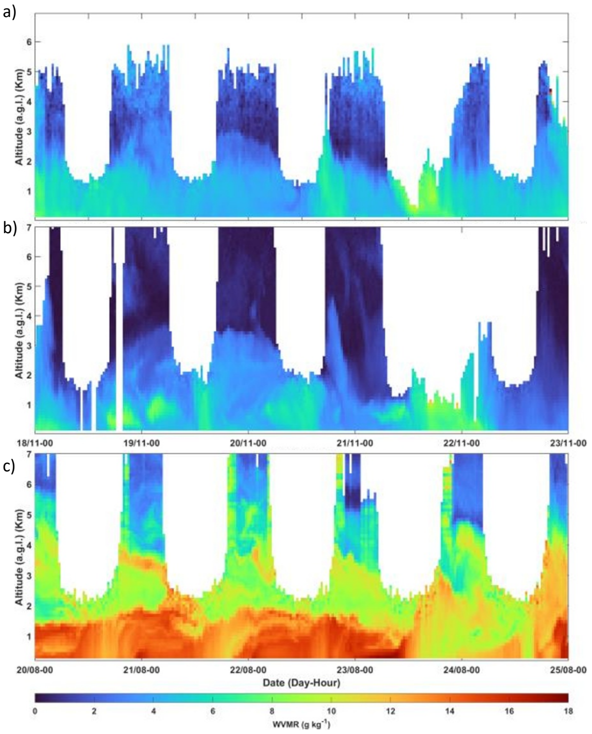

Fig. 4. Examples of the temporal evolution of WVMR vertical profiles derived from the Raman lidar as a function of altitude a.g.l. for a) HORUS–1, b) WALI and c) HORUS–2. The vertical resolution is 100 m and the time resolution is 30 min. The white area corresponds to low quality WVMR retrieval.

Examples of the temporal evolution of the WVMR during the WaLiNeAs campaign are shown in Figure 4. Figures a) and b) were taken in autumn 2022 in Grau du Roi and Cannes, respectively. Due to the proximity of the two sites (Fig. 1), there are similarities between the two figures. Figure c) was taken in summer 2023 in Toulouse, during an intense heatwave with temperature records. The atmosphere was very humid, even at high altitudes, with water vapor contents comparable to tropical levels. All data are archived in the AERIS database [9].

2.2 Uncertainties

For all three lidars, the contributions of the main bias and uncertainties sources are shown in Table 1 and Table 2, respectively. The bias that has the greatest impact on the signal is due to the calibration. The higher root mean square differences (RMSD) are encountered during daytime. They limit the altitude range of lidars at less than 2 km above ground level (a.g.l.). Throughout the measurement campaign, the planetary boundary layer cycle was fully sampled. During the night, the advections of humid air masses were clearly visible. We know that these humid layers play an important role in the development of convective systems by providing the latent heat needed to amplify deep convection to the upper troposphere.

Table 1. biases impacting lidar measurements.

Bias source		Bias value
Molecular contribution		< 0.1 %
Aerosols contribution		< 0.7 %
High voltage variation		1 – 2 %
Meteorological probe uncertainty		0.2 g kg^{-1}
Calibration	WALI	3.8 %
	HORUS–1	4.4 %
	HORUS–2	2.7 %

Table 2. Maximal root mean square difference (RMSD) due to i) the shot noise and ii) the shot noise and the atmospheric variability during both nighttime and daytime. Uncertainties are given for different altitude ranges and for each lidar. Vertical and temporal resolution of lidar profiles considered are 100 m and 15 min, respectively.

Lidar / RMSD	WALI	HORUS–1	HORUS–2
	0.03 g kg^{-1} (0 – 2 km)	0.07 g kg^{-1} (0 –2 km)	0.05 g kg^{-1} (0 – 5 km)

Nighttime	Shot noise	0.05 g kg^{-1} (2 – 5 km) 0.3 g kg^{-1} (5 – 10 km)	0.4 g kg^{-1} (2 – 4 km) 1 g kg^{-1} (4 – 5.5 km)	0.2 g kg^{-1} (5 – 10 km)
	Total	0.05 g kg^{-1} (0 – 2 km) 0.05 g kg^{-1} (2 – 5 km) 0.3 g kg^{-1} (5 – 10 km)	0.1 g kg^{-1} (0 –2 km) 0.4 g kg^{-1} (2 – 4 km) 1 g kg^{-1} (4 – 5.5 km)	0.1 g kg^{-1} (0 – 5 km) 0.2 g kg^{-1} (5 – 10 km)
Daytime	Shot noise	0.2 g kg^{-1} (0 –1.5 km) 1 g kg^{-1} (1.5 – 2 km)	0.3 g kg^{-1} (0 –1 km) 1 g kg^{-1} (1 – 1.5 km)	0.1 g kg^{-1} (0 –1.6 km) 0.3 g kg^{-1} (1.6 – 2.5 km)
	Total	0.4 g kg^{-1} (0 –1.5 km) 1 g kg^{-1} (1.5 – 2 km)	0.4 g kg^{-1} (0 –1 km) 1 g kg^{-1} (1 – 1.5 km)	0.4 g kg^{-1} (0 –1.6 km) 2 g kg^{-1} (1.6 – 2.5 km)

3 CONCLUSION

Thanks to their high temporal and spatial resolution, Raman lidars can be used to study the evolution of water vapor in the lower troposphere with a high degree of resolution. As part of the WaLiNeAs program, the assimilation of spatially and temporally resolved lidar data into mesoscale models is intended to improve the prediction of extreme events that can occur in the western Mediterranean basin, an area that will be increasingly exposed to extreme events owing to global warming.

ACKNOWLEDGEMENTS

Friendly acknowledgements to local authorities of Port Camargue harbor master's office, Thales-Alenia-Space, the town of Coursan and the Météo-France centre in Toulouse. This research has been supported by the Agence Nationale de la Recherche via the WaLiNeAs project (grant no. ANR-20-CE04-0001).

References

[1] Giorgi, F. and Lionello, P.: Climate change projections for the Mediterranean region, Glob Planet Change, 63, https://doi.org/10.1016/j.gloplacha.2007.09.005, 2008.

[2] Ricard, D., Ducrocq, V., and Auger, L.: A climatology of the mesoscale environment associated with heavily precipitating events over a northwestern Mediterranean area, J Appl Meteorol Climatol, 51, https://doi.org/10.1175/JAMC-D-11-017.1, 2012.

[3] Duffourg, F. and Ducrocq, V.: Origin of the moisture feeding the heavy precipitating systems over southeastern France, Natural Hazards and Earth System Science, 11, https://doi.org/10.5194/nhess-11-1163-2011, 2011.

[4] Flamant, C., Chazette, P., Caumont, O., Di Girolamo, P., Behrendt, A., Sicard, M., Totems, J., Lange, D., Fourrié, N., Brousseau, P., Augros, C., Baron, A., Cacciani, M., Comerón, A., De Rosa, B., Ducrocq, V., Genau, P., Labatut, L., Muñoz-Porcar, C., Rodríguez-Gómez, A., Summa, D., Thundathil, R., and Wulfmeyer, V.: A network of water vapor Raman lidars for improving heavy precipitation forecasting in southern France: introducing the WaLiNeAs initiative, Bulletin of Atmospheric Science and Technology, 2, https://doi.org/10.1007/s42865-021-00037-6, 2021.

[5] Chazette, P., Flamant, C., Raut, J. C., Totems, J., and Shang, X.: Tropical moisture enriched storm tracks over the Mediterranean and their link with intense rainfall in the Cevennes-Vivarais area during HyMeX, Quarterly Journal of the Royal Meteorological Society, 142, https://doi.org/10.1002/qj.2674, 2016.

[6] Laly et al. (2024): Water vapor Raman-lidar observations from multiple sites in the framework of WaLiNeAs, https://doi.org/10.25326/537

[7] Chazette, P., Marnas, F., and Totems, J.: The mobile Water vapor Aerosol Raman LIdar and its implication in the framework of the HyMeX and ChArMEx programs: Application to a dust transport process, Atmos Meas Tech, 7, 1629–1647, https://doi.org/10.5194/amt-7-1629-2014, 2014b.

[8] Totems, J., Chazette, P., and Baron, A.: Mitigation of bias sources for atmospheric temperature and humidity in the mobile Raman Weather and Aerosol Lidar (WALI), Atmos Meas Tech, 14, 7525–7544, https://doi.org/10.5194/amt-14-7525-2021, 2021.

[9] Chazette, P., Laly, F., Totems, J. & Lagarrigue, J.: WaLiNeAs France. [Dataset]. Aeris. https://doi.org/10.25326/537, 2023.